Thermodynamic and Structural Study of the Copper-Aluminum System by the Electrochemical Method Using a Copper-Selective Beta# Alumina Membrane

As Published: https://doi.org/10.1007/s11663-018-1400-y

Publisher: Springer US

Persistent URL: https://hdl.handle.net/1721.1/131897

Version: Author's final manuscript: final author's manuscript post peer review, without publisher's formatting or copy editing

Thermodynamic and Structural Study of the Copper - Aluminium System by the Electrochemical Method Using a Copper-Selective Beta" Alumina Membrane

Caspar Stinn[1,2], Antoine Allanore[2]*

[1] Massachusetts Institute of Technology, Department of Chemical Engineering
Cambridge, MA 02139
[2] Massachusetts Institute of Technology, Department of Materials Science and Engineering
Cambridge, MA 02139
* Corresponding author, allanore@mit.edu

Abstract

The liquid phase thermodynamic of mixing of the copper-aluminium binary system is investigated as a function of temperature and composition using the electrochemical potential difference method. A copper-selective beta" alumina (Cuβ"Al_2O_3) is used as a solid electrolyte, synthesized through ion exchange, sintering from base oxide powders, and the floating zone method of crystal growth. Measured thermodynamic of mixing data were used to inform short range ordering in copper-aluminium melts through Darken's factor for excess stability and Bhatia-Thornton structure factors, revealing a strong departure from ideality and pronounced ordering. Mixing properties were used to predict viscosity and self-diffusion coefficients. Features observed in calculated electronic entropy of mixing for copper-aluminium were compared to trends in viscosity, demonstrating the utility of electronic property of mixing in the description of structure-properties in this liquid binary system.

Introduction

The copper-aluminium binary system remains industrially critical due to the prevalence of copper as an alloying agent for aluminum and a base metal for aluminium bronze products. In the aluminium industry, the addition of copper enables precipitation hardening and heat treatment[1] in 2XXX series alloys, and increases strength in 2XXX and 6XXX alloys[2]. Conversely, aluminium bronzes have long been utilized for corrosion resistant applications[3], and remain an active area of research for high strength and wear resistant alloys[4]. All of those products are processed via the molten state, and require a careful mastering of the concentration and distribution of copper in both the liquid state and during solidification. Examples of the corresponding processing issues include macrosegregation[5] or control of the copper content when using recycled feeds[6,7].

Indeed, despite the prevalence of copper-aluminium alloys in industrial applications, liquid phase phenomena remain uncertain starting from inconsistencies in models for copper-aluminium thermodynamics[8–14] and melt structure[15–18]. In addition, while physical properties such as density, viscosity, and surface tension of copper-aluminium melts have received experimental attention[13,19–22], such quantities are difficult to measure accurately for molten aluminium alloys[19] and limited effort is found to relate these properties to accurate experimental thermodynamics of mixing data. While molecular dynamics simulations[15–18,23–26] have attempted to elucidate the relation between thermodynamic, structural, and physical properties for the copper-aluminium system, the efficacy of available computational approaches is hindered by a lack of experimental data for comparison.

An electrochemical study of the copper-aluminium system is herein investigated, with the objective to inform the free energy and entropic thermodynamic of mixing of the liquid binary system. Consequently, thermodynamics of mixing properties are used to inform the structural and transport properties of the melt.

To study the thermodynamic behavior of the copper-aluminium system, the use of a copper-selective, alumina-based solid electrolyte is proposed. Beta (β) and beta" (β") alumina solid electrolytes (BASE) have been extensively investigated for use in high temperature

electrochemical applications due to their thermal stability, low electronic conductivity, and high and selective ionic conductivity. Most BASE studies and applications thus far have targeted sodium and lithium ion conducting solid electrolytes, with far less attention given to BASE exhibiting ionic transport of other species. Sodium ion conducting BASE have found applications in energy storage, such as in the sodium-sulfur battery[27], thermoelectric devices[28,29], and heat engines[30,31]. Sodium-selective BASE have also been demonstrated for use in both liquid and vapor sensors[32–34], illustrating their potential use for thermodynamic sensing applications in industrial processes.

A variety of methods, ranging from powder sintering[35,36] to the Czochralski method of crystal growth[37], have been established for the preparation of BASE with sodium ion transport properties (Naβ"Al_2O_3). Naβ"Al_2O_3 is traditionally used to synthetize BASE which are selective for other ions[35,38–41] via ion exchange. One copper-selective BASE previously reported is copper (I) β" alumina (Cuβ"Al_2O_3) [42]. Cuβ"Al_2O_3 solid electrolyte has previously been synthesized but has thus far seen limited application. Currently, its only application is electrochemical potential measurements for liquid copper-nickel[43] and copper-tin[44] thermodynamic of mixing. Cuβ"Al_2O_3 has also been suggested as a candidate material for tunable solid-state lasers[45]. However, potential applications of Cuβ"Al_2O_3 in liquid metal processing and chemical sensors, for which other BASE have been applied[32–34], have thus far been largely ignored. Nevertheless, Cuβ"Al_2O_3 presents a promising material for use in measuring the thermodynamics of mixing for the copper-aluminium system.

In this study, Cuβ"Al_2O_3 is utilized as a solid electrolyte for high temperature thermodynamic measurements in the copper-aluminium system using the electrochemical potential difference (formerly known as EMF) method[32,33,43,44,46–48]. The following isothermal electrochemical cell has been constructed:

$$Cu - Al|Cu\beta"Al_2O_3|Cu \quad (1)$$

Depending on the temperature the right compartment of the cell may be solid or liquid, while the thermodynamic reference state utilized here for copper is liquid copper at the temperature of interest (molar Gibbs energy of pure liquid copper, μ_{Cu}^{ref}). With the goal to inform the thermodynamic mixing properties of the liquid binary Cu-Al, one relates the chemical potential of copper in the binary solution (or partial molar Gibbs energy, $\mu_{\underline{Cu}}$) to the cell potential difference (E), using the Nernst equation:

$$\mu_{\underline{Cu}} - \mu_{Cu}^{ref} = zFE \quad (2)$$

where z is the number of electrons per copper (I) ion that travels across the Cuβ"Al_2O_3 membrane ($z = 1$), R is the ideal gas constant, T is the absolute temperature and F is Faraday's constant. All other thermodynamic functions of mixing can be calculated from the experimental cell potential (E) variation with composition or temperature, as presented in [48]. For example, copper activity in the selected reference state is calculated at each composition from the cell potential via:

$$a_{Cu(in\ Al)} = e^{\frac{zFE+\mu_{Cu}^{ref}}{RT}} \quad (3)$$

A linear fitting of the variation of the cell potential with temperature at a fixed composition provides estimates of the partial molar enthalpy ($\bar{H}_{Cu}$) and partial molar entropy ($\bar{S}_{Cu}$) for copper following Gibbs–Helmholtz[48]:

$$E = \frac{-\bar{H}_{Cu}}{zF} + \frac{T\bar{S}_{Cu}}{zF} \quad (4)$$

The corresponding partial molar properties of aluminum can be calculated by integration of the Gibbs-Duhem equation[49], where x denotes mole fraction and Y denotes entropy, enthalpy, or Gibbs energy:

$$\bar{Y}_{Al} = -\int \frac{x_{Cu}}{x_{Al}} \left(\frac{d\bar{Y}_{Cu}}{dx_{Cu}}\right) dx_{Cu} \quad (5)$$

In the present work, the integration was conducted numerically from a smoothed-spline interpolation of $\bar{Y}_{Cu}$ with x_{Cu}.

To inform the liquid phase structure necessary to accurately model the thermodynamics of a liquid binary system, Darken's factor for excess stability (ES) has been proposed[50]. It is evaluated from the excess properties of mixing as shown in Eqn(6):

$$ES = \frac{\partial^2\left(\Delta H^M - T\Delta S_{Excess}^M\right)}{\partial {x_{Cu}}^2} \quad (6)$$

ΔH^M is the enthalpy of mixing, and ΔS_{Excess}^M is the excess entropy of mixing from measured entropy of mixing (ΔS^M) and the ideal configurational entropy of mixing, ΔS_{Ideal}^M:

$$\Delta S_{Excess}^M = \Delta S^M - \Delta S_{Ideal}^M \quad (7)$$

For ideal or near ideal liquid alloys, excess stability typically decreases monotonically as a function of x_{Cu}. The function will show peaks where strong chemical interactions occur centered on the stoichiometry of associate complexes[50,51]. Utilizing excess stability, the Bhatia-Thornton structure factor in the long wavelength limit, $S_{CC}(0)$, can be calculated[50]:

$$S_{CC}(0) = \frac{RT}{\frac{RT}{x_{Cu}x_{Al}} + ES} \quad (8)$$

For an ideal solution, the Bhatia-Thornton structure factor in the long wavelength limit is equal to the following:

$$S_{CC}(0) = x_{Cu}x_{Al} \quad (9)$$

The height and width of dips in the calculated Bhatia-Thornton structure factor with composition across the binary, compared to the ideal case, provide further insight into the extent of ordering.

As shown and defined recently[52], electronic state entropy can also reflect short-range ordering. For systems in which the Drude model applies, electronic entropy of mixing (ΔS_e^M)

can be calculated as follows, where S^e is the electronic entropy, R_H is the Hall Effect coefficient, m is the Hall mobility, σ is the electrical conductivity, and α is the Seebeck coefficient:

$$S^e = \frac{|\alpha|}{R_H} = \frac{|\alpha|\sigma}{m} \tag{10}$$

$$\Delta S_e^M = S_{Cu-Al}^e - x_{Cu}S_{Cu}^e - x_{Al}S_{Al}^e \tag{11}$$

Minima in the electronic entropy of mixing have previously proven to correspond to ordering, similar to associate complexes. In addition to an advanced description of the thermodynamics of mixing, insight into liquid metal structure is necessary to select suitable models for the evaluation of the physical properties.

Indeed, measured thermodynamics of mixing can be used to predict physical properties such as viscosity. Previously, Eyring proposed that viscosity was the result of kinetic phenomena, and could be modeled by an Arrhenius-type equation[53], where η is the dynamic viscosity, η^∞ is a pre-exponential term, and E^A is the activation energy for viscous flow:

$$\eta = \eta^\infty e^{\frac{E^A}{RT}} \tag{12}$$

Numerous semi-empirical models have been proposed to calculate η^∞ and E^A for binary alloy systems from thermodynamics of mixing data[13,54–56]. For non-ideal systems the Kozlov model has shown to be suitable[56] for calculation of η^∞ and E^A as follows:

$$\eta_{Cu-Al}^\infty = e^{x_{Cu}\ln\eta_{Cu} + x_{Al}\ln\eta_{Al}} \tag{13}$$

$$E_{Cu-Al}^A = -\frac{1}{3}\Delta H^M \tag{14}$$

Another relevant viscosity model is the Schick-Brillo model[13], originally derived from CALPHAD models of the copper-aluminium system published at the time, which assumed excess entropic effects were minimal. E_i^A and η_i^∞ of the pure end members are determined from the viscous flow activation energies and pre-exponentials calculated from experimental data[22] using fits to Eqn(12). E_{i-j}^A and η_{i-j}^∞ for the Schick-Brillo model can then be calculated using the following equations[13]:

$$\eta_{Cu-Al}^\infty = e^{x_{Cu}\ln(x_{Cu}\eta_{Cu}^\infty) + x_{Al}\ln(x_{Al}\eta_{Al}^\infty)} \tag{15}$$

$$E_{Cu-Al}^A = x_{Cu}E_{Cu}^A + x_{Al}E_{Al}^A - \Delta H^M \tag{16}$$

The determination of viscosity in binary melts facilitates further characterization of transport phenomena. Dynamic viscosity coupled with activity data can be used to calculate self-diffusion coefficients, D, for copper and aluminum within the melts as follows using the Singh-Sommer relation[57], where c is the molar concentration, k_B is Boltzmann's constant, and r is the radius of the diffusing particle:

$$D_{Cu} = \frac{k_B T}{6\pi\eta r_{Cu}} \frac{d\ln a_{Cu}}{d\ln c_{Cu}} \tag{17}$$

$$D_{Al} = \frac{k_B T}{6\pi\eta r_{Al}} \frac{d \ln a_{Al}}{d \ln c_{Al}} \quad (18)$$

Experimental access to thermodynamic mixing properties is therefore critical to enable a full characterization of the structure and transport properties of the binary liquid Al-Cu systems. Electrochemical potential difference data the liquid copper-aluminium system acquired through the use of copper-selective membrane are herein seek for, as a first step to increase the accuracy in the modelling and prediction of thermodynamic and physical properties of such melt. In this paper, the use of Cuβ"Al_2O for the copper-aluminium system in such context is presented, from synthesis to experimental application. We demonstrate that Cuβ"Al_2O_3 can be readily synthesized through both sintering and melt-based routes for use as a solid electrolyte. We report the first electrochemical measurements of mixing thermodynamics data for the liquid binary Cu-Al using Cuβ"Al_2O_3. Those results are complemented with calculations of the electronic state entropy of mixing. These complementary results support a discussion of available thermodynamic models and their relations to the prediction of viscosity and diffusivity, indicating the possible utility of electronic entropy of mixing in the context of relating ordering and structure for such alloy system.

Methods

Three synthesis methods for copper(I) β" alumina (Cuβ"Al_2O_3) were investigated in this work. The method of synthesis that minimized cracking and maximized density of the solid electrolyte was utilized to fabricate Cuβ"Al_2O_3 for use in electrochemical cells to measure copper – aluminium mixing thermodynamics [32,33,43,44,46–48]

Synthesis of Copper(I) β" Alumina

Copper(I) β" alumina (Cuβ"Al_2O_3) of composition $Cu_5Mg_2Al_{31}O_{51}$ was synthesized using 1) ion exchange from sodium β" alumina (Naβ"Al_2O_3), following similar methods to Fray et al.[42], 2) direct sintering from the base oxides, or 3) from an oxide melt through the floating zone method of crystal growth[58].

1) Ion exchange from Naβ"Al_2O_3[42]

One method of synthesis of copper(I) β" alumina (Cuβ"Al_2O_3) is through exchange of sodium with copper from sodium β" alumina (Naβ"Al_2O_3)[42,43]. Using copper chloride as the exchange medium at both the working (WE) and counter (CE) electrode, the following reactions occur:

$$WE: 2CuCl + 2Na\beta"Al_2O_3 \leftrightarrow Cl_2 + 2Na^+ + 2Cu^+ + 2\beta"Al_2O_3{}^- + 2e^- \quad (19)$$

$$CE: Cl_2 + 2Na^+ + 2Cu^+ + 2\beta"Al_2O_3{}^- + 2e^- \leftrightarrow 2NaCl + 2Cu\beta"Al_2O_3 \quad (20)$$

The overall cell reaction for the ion exchange is:

$$CuCl + Na\beta"Al_2O_3 \leftrightarrow NaCl + Cu\beta"Al_2O_3 \quad (21)$$

Disks of Naβ"Al_2O_3 of stoichiometry $Na_5Mg_2Al_{31}O_{51}$ were synthetize from sodium aluminium oxide ($Al_2O_3 \cdot Na_2O$, tech purity, Alfa Aesar), magnesium oxide (MgO, 99.95% pure

metals basis, Alfa Aesar), and aluminium oxide (99.95% pure metals basis, Alfa Aesar) in a 5:2:13 formula unit ratio. The powders were then held in a vacuum oven at 473 K (200 °C) for 2 hours, mixed in a micronizing mill for 2 hours, and isostatically pressed into disks (∅19 mm, ∅6 mm, length 10 – 25 mm). Isostatic pressures of 100 – 600 MPa were tested. The disks were sealed using alumina paste in alumina tubes filled with extra sodium β" alumina powder to suppress vaporization of sodium oxide during sintering, then sintered under air in a tube furnace. Temperatures ranging from 1673 K – 2073 K (1400 °C – 1800 °C) were explored. Copper(I) chloride (CuCl, 97%, Sigma Aldrich) was used for ion exchange, where a Naβ"Al_2O_3 pellet is the solid electrolyte separating two pools of copper(I) chloride (Figure 1) held at 823 K (550 °C) under argon (99.95% purity, Airgas) at a flowrate of 50 cm^3/min. A potential difference of 500 mV was applied using graphite electrical leads using a potentiostat (Gamry Instruments, Reference 3000). The potential difference was applied until 150% of the theoretical charge to exchange the sodium with copper had passed. The exchanged Cuβ"Al_2O_3 was cleaned of residual CuCl by submerging the pellet in nitric acid (70 wt%, Sigma Aldrich) for 1 minute.

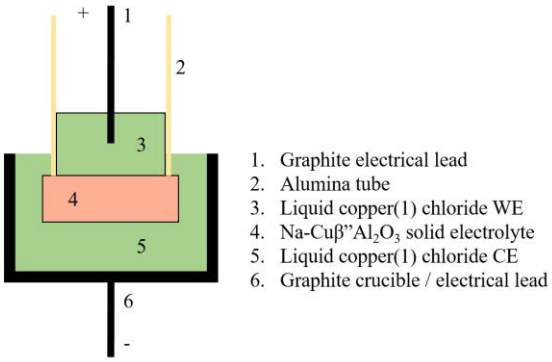

Figure 1: Electrochemical cell for exchange of Na^+ with Cu^+ in β"-Al_2O_3

2) Direct sintering from the base oxides.

Sintered disks of Cuβ"Al_2O_3 were synthesized[42] directly from copper(I) oxide (Cu_2O, 97% pure, Sigma-Aldrich), magnesium oxide (MgO, 99.95% pure metals basis, Alfa Aesar), and aluminium oxide (99.95% pure metals basis, Alfa Aesar) in a 5:4:31 formula unit ratio mixed in a micronizing mill for 2 hours. Disks (∅19 mm, ∅38 mm, length 1 – 20 mm) were isostatically pressed and then sintered in a box furnace under air for three hours, with heating and cooling rates of 5 K/min. Isostatic pressures and sintering temperatures ranging from 100 – 600 MPa and 1673 K – 2073 K (1400 °C – 1800 °C) respectively were explored.

3) Direct crystal growth using a floating zone furnace [58]

Cuβ"Al_2O_3 was also synthesized directly through zone melting in a floating zone optical furnace (Crystal Systems Corporation, TX-12000-I-MIT-VPO-PC) using the floating zone method of crystal growth[58]. Rods of polycrystalline copper(I) β" alumina (∅8 mm, length 100 mm) synthesized using the method 2 described above were suspended in the hot zone of the furnace, 1 mm above an alumina rod (∅8 mm). The rods were spun in opposite directions at speeds of 10 rpm. The tip of the Cuβ"Al_2O_3 rod was melted at 18% furnace power under air, forming a droplet which subsequently joined to the alumina rod, resulting in a suspended molten region of Cuβ"Al_2O_3 bridging the alumina and

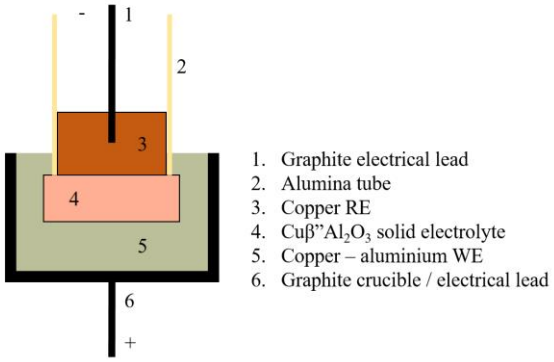

Figure 2: Electrochemical potential measurement cell - geometry 1

sintered Cuβ"Al_2O_3 rods. The rods were moved through the furnace hot-zone in unison at a rate of 10 mm/hour, with the sintered Cuβ"Al_2O_3 rod being melted and solidified onto the alumina rod. After 60mm of travel through the floating zone furnace hot zone, the vertical movements of the rods were stopped and the rods were cooled by decreasing the lamp power at a rate of 6% per hour.

Copper – aluminium alloy samples across the entire composition range were prepared from copper shot (99.999% pure metals basis, Alfa Aesar) and aluminium (99.99% pure metals basis, Alfa Aesar). Samples were pre-melted in a tube furnace under argon (99.95% purity, Airgas) at a flowrate of 50 cm^3/min) at 1473 K (1200 °C) for 3 hours to ensure homogeneity. All EMF experiments were also performed in tube furnaces under argon (99.95% purity, Airgas) at a flowrate of 50 cm^3/min.

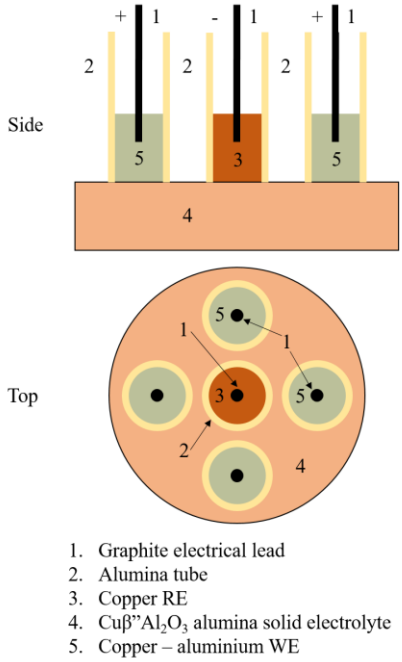

Figure 3: Electrochemical potential measurement cell - geometry 2

Two cell geometries were investigated. Geometry 1 (Figure 2) consisted of a Cuβ"Al_2O_3 pellet (∅12 mm, thickness 3 mm) joined to an alumina tube (OD 9.5mm, ID 6.5mm) with alumina paste, forming a vessel which contained the copper reference (REF) electrode (99.999% pure metals basis, Alfa Aesar) and a graphite electrical lead. This vessel was submerged in a copper – aluminium sample of known composition held in a graphite crucible, with the graphite crucible serving as the electrical lead (working electrode, WE).

Geometry 2 (Figure 3) consisted of a Cuβ"Al_2O_3 disk (∅38 mm, thickness 3 mm), onto which alumina tubes (OD 9.5mm, ID 6.5mm) were joined with alumina paste to hold the sample and reference melts. Graphite electrodes were utilized.

The cell potential difference was determined by measuring the open circuit potential (OCP) of the copper-aluminium sample (WE) versus pure copper (REF) across the Cuβ"Al_2O_3 membrane using a potentiostat at an acquisition frequency of 10 hz (Gamry Instruments, Reference 3000). The cell was held at temperature for 1800 seconds before a measurement was taken, ensuring a steady OCP reading.

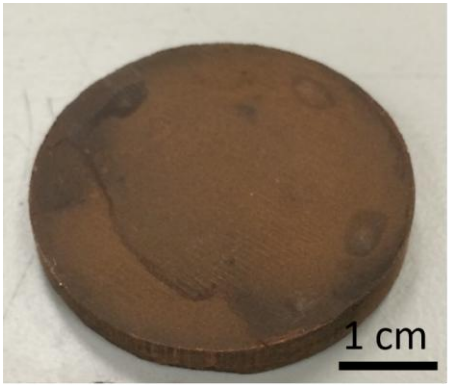

Figure 4: Cuβ"Al_2O_3 synthesized directly from Cu_2O, MgO, and Al_2O_3 powders sintering

Results

Synthesis of Copper(I) β" Alumina

Copper(I) β" alumina (Cuβ"Al_2O_3) was successfully synthesized through each of the three methods. The target stoichiometry of $Cu_5Mg_2Al_{31}O_{51}$ was verified using scanning electron microscopy (SEM, JEOL JSM-6610LV, JEOL Ltd.) equipped with an energy dispersion spectroscopy analyzer

(EDS, Sirius SD detector, SGX Sensortech Ltd.) Direct preparation from sintering of copper(I) oxide, alumina, and magnesia (method 2) was found to be the easiest route of synthesis resulting in densified solid electrolytes free of visible macroscopic cracking. Densities were measured using ethanol displacement.

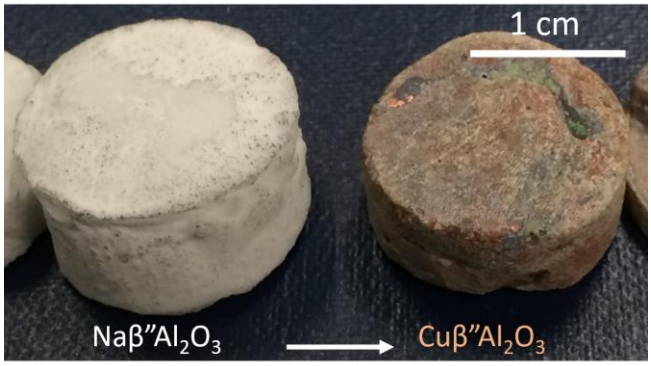

Figure 5: Cuβ”Al_2O_3 synthesized through ion exchange with Naβ”Al_2O_3, synthesized from $NaAlO_2$, MgO, and Al_2O_3 sintering

For the preparation of Cuβ”Al_2O_3 from base oxide sintering (method 2), a pressing pressure of 120 MPa, a green body thickness of 4mm and a sintering temperature of 1773 K (1500 °C) were found to maximize density and minimize cracking of the solid electrolyte. Sintered product densities of 3.4 – 3.5 g/cm^3 were achieved. The Cuβ”Al_2O_3 was not observed to be air sensitive. Machining of the sintered material was found to be similar to that of alumina. The color was observed to be a dark pinkish-brown (Figure 4).

In the synthesis of Naβ”Al_2O_3 for ion-exchange for method 1, isostatic pressing pressure of 450 MPa, green body thickness of 6mm, and a sintering temperature of 1973 K (1700 °C) were found to maximize density and minimize cracking. The corresponding sintered densities were in the range of 3.0-3.2 g/cm^3. After preparation, the Naβ”Al_2O_3 had to be kept under nitrogen, as large cracks formed over the course of a week if left in air. The Naβ”Al_2O_3 was more brittle in machining than pure alumina. During ion exchange to Cuβ”Al_2O_3, average current densities of 75 A/m^2 were observed at 823 K. SEM/EDS analysis showed conversion to Cuβ”Al_2O_3 to be greater than 99%. Following ion exchange, the Cuβ”Al_2O_3 showed similar physical properties to that synthesized from direct sintering from the base oxides (Figure 5).

Figure 6: Cuβ”Al_2O_3 synthesized directly from melt of Cu_2O, MgO, and Al_2O_3

Prepared from the melt (method 3), Cuβ”Al_2O_3 was observed to have a density of 3.5 g/cm^3, and be a nearly-opaque, reddish-black color (Figure 6). Approximately 2 cm of movement through the furnace hot zone was required for the resulting Cuβ”Al_2O_3 to appear uniform in diameter and composition. Rods of Cuβ”Al_2O_3 were found to fracture easily.

Thermodynamic Study of the Copper – Aluminium System

Cuβ”Al_2O_3 was utilized to measure the mixing thermodynamics of the copper-aluminium binary system through electrochemical method. When used to study a copper-aluminium alloy of 10 wt% copper, Cuβ”Al_2O_3 synthesized through all methods were found to perform equally in the temperature range of interest, 821 K to 1563 K (548 °C to 1290 °C). As a result, Cuβ”Al_2O_3 made directly from sintering of copper(I) oxide, alumina, and magnesia (Method 2) was used for all measurements, since its synthesis was the most straightforward. Both cell geometries 1 and 2

were also found to function equally, with open circuit potentials reaching steady state within 30 minutes and subsequently remaining stable over time (Appendix 1).

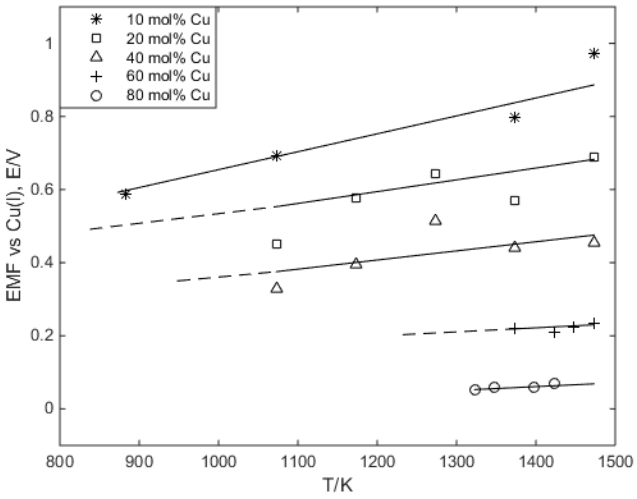

Figure 7: Variation of the electrochemical potential, referenced to liquid copper, with temperature and for 5 compositions (solid lines shows reproducible temperature range, dashed lines extend to the liquidus reported in [59])

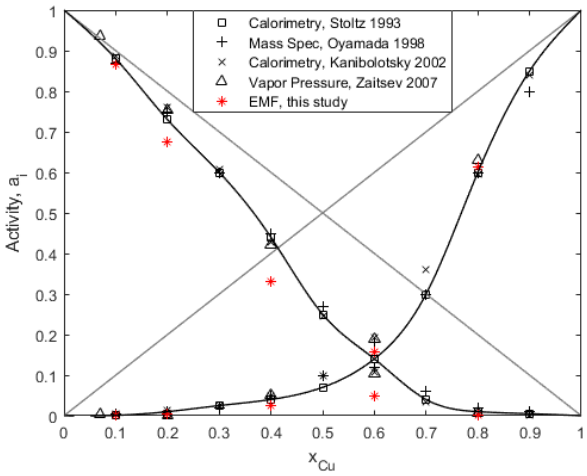

Figure 8: Copper and aluminium activity evaluated at 1373K, compared to literature values [9-12]. Lines are spline fit interpolation of the present data, and aluminium activity estimated from Gibbs-Duhem eqn(5).

Steady-state EMF measurements for five compositions in the binary copper-aluminium liquid phase reported in the phase diagram published by Murray[59] are presented in Figure 7 as a function of temperature. Only for copper contents of 10 mol% and 80 mol% could stable cell potential be measured from 1473K (1200 °C) down to the liquidus points, 873 K and 1318 K respectively (600 °C and 1045 °C), reported in [59].

For copper compositions exceeding 10 mol% and less than 80 mol%, signals failed to stabilize for temperatures around 200 K from the liquidus. EMF data were fitted linearly in this temperature range, using Eqn(7) to determine partial molar enthalpy and entropy. The corresponding activities of copper and aluminum at 1373 K (1100 °C) calculated using Eqn(6) are presented in Figure 8, and compared to literature values obtained by other methods [9–12]. The copper activity agreement is found to be acceptable at the single previously-studied temperature of 1373 K, falling within the range of literature values[9–12] for all compositions studied except for 40 mol%, for which the electrochemical data underestimated the activity by 45%. Aluminium activity predicted from electrochemical data using Eqn(8) systematically underestimated the literature values[9–11] by 15, 25, and 50% at compositions of 20, 40, and 60 mol% Cu respectively, arising from numerical error in fitting the data for the Gibbs-Duhem integration (Eqn 5). Study of additional compositions would support greater accuracy for the Gibbs-Duhem numerical integration, though clear trends can already be noticed.

With the aim to support structure/properties relationship, integral Gibbs energy, enthalpy, and entropy of mixing are depicted in Figures 9-11. Spline fit interpolations were utilized to construct curves following a recent study that suggested such numerical interpolation provides a more accurate fitting to chemical potential functions than polynomial fits.[60] A table

summarizing all thermodynamic data is included in Appendix 2. Previously reported peak experimental values for enthalpy of mixing range from -4.5 kJ/mol[61] to -18 kJ/mol[9,11,12]. Our peak enthalpy of mixing is in close agreement with that presented [44] by Kubaschewski and Alcock. Excess entropy at 50 mol% Cu was found to be 50% higher than the estimation also reported in [44].

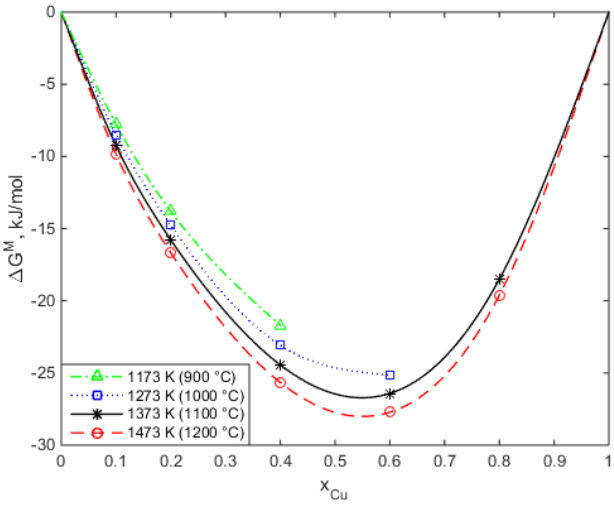

Figure 9: Gibbs energy of mixing estimated from electrochemical potential data (lines are spline fit interpolations)

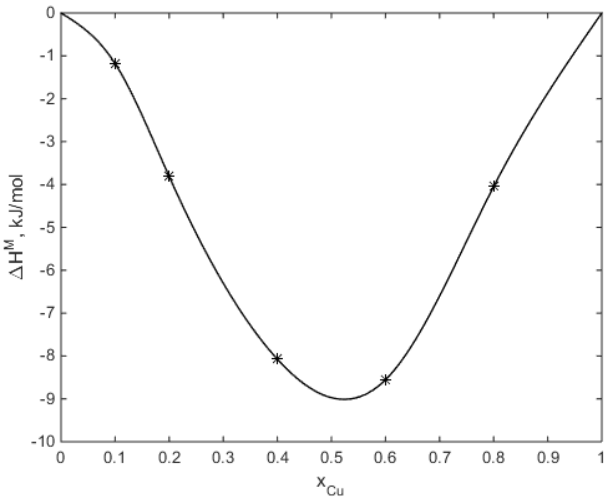

Figure 10: Enthalpy of mixing at 1373 K (1100 °C) calculated by fitting the potential data to the Gibbs-Helmoltz relation (line is a spline fit interpolation)

Overall, the close relation of our results to prior experimental art demonstrates that electrochemical methods utilizing Cuβ”Al_2O_3 can be applied to systems with thermodynamically-complicated liquid phases to directly determine activity, Gibbs energy, enthalpy, and entropy of the liquid alloy. Difficulty in measuring EMF near the liquidus for alloys of intermediate copper composition is also believed to be caused by short range ordering effects at the interface between the liquid alloy and the solid-electrolyte.

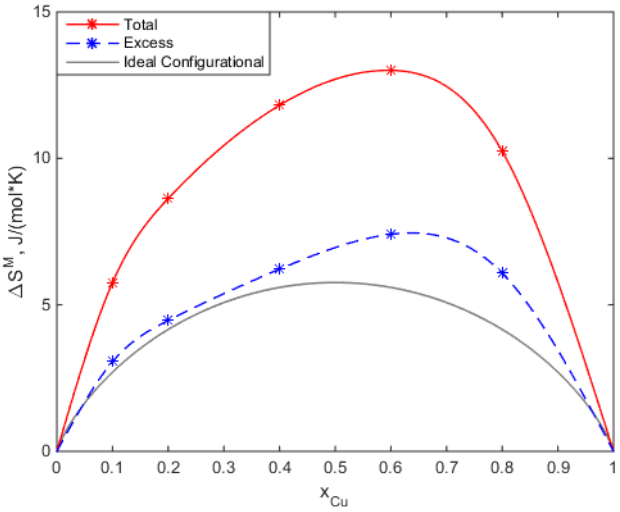

Figure 11: Total (stars, plain line) and excess (stars, dashed line) entropy of mixing at 1373 K (1100 °C) calculated by fitting the potential data to the Gibbs-Helmoltz relation (lines are spline fit interpolation). Plain

curve is the ideal entropy of mixing

Discussion

Throughout the temperature range studied, the binary liquid activities exhibit strong negative deviations from ideality. The negative Gibbs energy of mixing is caused by contributions from both excess entropy of mixing and exothermic enthalpy of mixing. Previously, Stolz predicted the non-ideal behavior of the copper-aluminium system to be driven by the existence of an $AlCu_2$ associate complex[12], whereas Zaitsev predicted AlCu and $AlCu_3$ associate complexes[9]. However, minimal experimental efforts, such as neutron diffraction measurements, have been directed at characterizing ordering in the copper-aluminium system.

Nevertheless, thermodynamics of mixing can be utilized to provide insight into the structure of liquids. Darken's factor for excess stability ES depicted in Figure 12 can be calculated using Eqn(6) [50]. As seen in Figure 12, a peak in excess stability is centered on $AlCu_2$, corroborating the prediction by Stolz[12]. The existence of ordering within the copper-aluminium system is reiterated through examination of the Bhatia Thornton structure factor. In the long wavelength limit, the Bhatia-Thornton structure factor $S_{CC}(0)$ can be calculated through Eqn(9) [50].

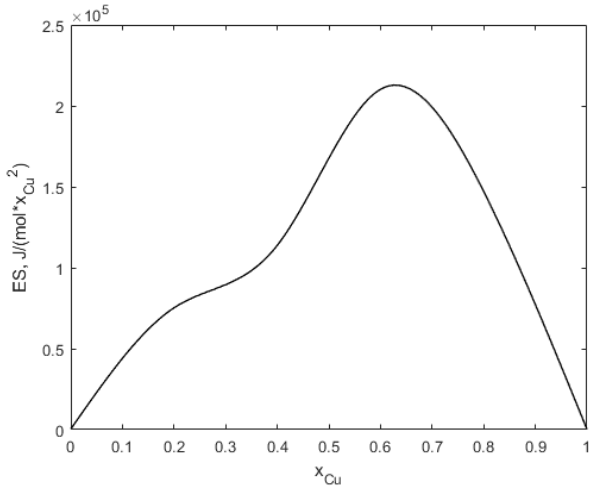

Figure 12: Excess stability (ES) calculated from experimentally determined thermodynamic properties of mixing, using Eqn(6) at 1373 K (1100 °C). Line is calculated from a spline fit interpolation of excess Gibbs energy of mixing

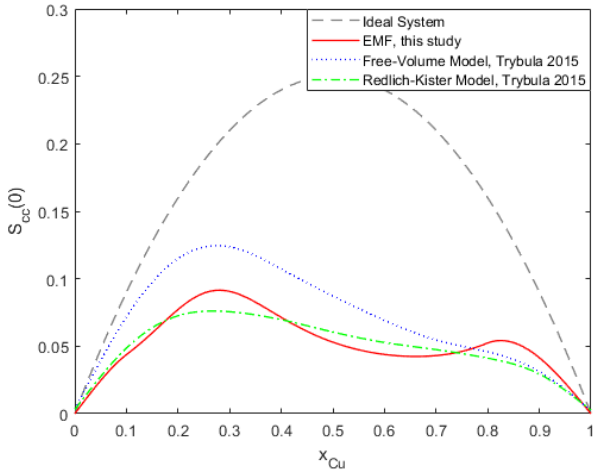

Figure 13: Bhatia-Thornton structure factor ($S_{CC}(0)$) at 1373 K (1100 °C) evaluated from the excess stability evaluated from the present data, compared to the ideal case using Eqn(8-9). Line is calculated from the spline fit interpolation utilized for excess stability. Dashed curves represent results of computational models [62]

As presented in Figure 13, $S_{CC}(0)$ shows a divergence from ideal behavior in copper contents above 30 mol% Cu, characteristic of strong ordering in the copper rich region of the phase diagram. The trough is centered on 66 mol% Cu, further suggesting the existence of an $AlCu_2$ associate complex. The composition range where ordering is observed from our results is in agreement with recent computational results.[62]

Nevertheless, upon the inspection of integral total Gibbs energy, enthalpy, and entropy of mixing curves (Figures 9-11), the true extent of ordering within the melt is not readily apparent. To better understand the role of ordering within the system, a more refined thermodynamic descriptions proves necessary. Previously, Rinzler and Allanore demonstrated the correlation between trends in electronic entropy of mixing and ordering within high temperature liquid binary systems[52]. Using electrical conductivity [63] (Figure 14), Seebeck[63], and Hall effect[64] data, electronic entropy of mixing can be calculated through Eqn(10-11). As neither Hall effect coefficients nor Hall mobility data are reported for the copper – aluminium binary, the Hall mobility was estimated from data for pure liquid copper and aluminium. Four scenarios were considered to evaluate the possible variation of those electronic properties as a function of composition, as presented in Figures 15 and 16. Case 1 assumed a linear variation of the Hall effect coefficient with mole fraction. Case 2 assumed a linear variation of the Hall mobility with mole fraction. Case 3 was based on the only systems for which such variation has been measured. Indeed, for Cu-Bi, Cu-Sb, Cu-Sn, and Cu-In liquid binary alloys, Takeuchi et al. [65] showed that the Hall effect coefficient was approximately the one of the non-copper end member from 0 to 70 mol% Cu, while linearly reaching the one of pure copper from 70mol% to pure copper. This scenario was taken to be Case 3. Case 4 was the opposite scenario from Case 3, where the Hall effect coefficient of the binary was taken to be the one of copper from 30 mol% Cu to pure copper and assuming a linear variation of the Hall effect coefficient from pure aluminium to 30 mol% Cu.

Remarkably, as shown in Figure 17, the shape and magnitude of the calculated electronic entropy of mixing proves resilient to uncertainty in the mobility term. A pronounced local minimum in the electronic entropy of mixing for the copper aluminium system is observed in the region of 50 mol% to 75 mol% Cu, reflecting the ordering present within the system. Other entropic features and local minima, masked in the overall and excess entropy of mixing curves are also visible. As presented in Figure 18, the composition of these minima mimic the inflections observed in viscosity trends. This correlation between viscosity and electronic entropy is not entirely surprising if both are considered reflecting short-range ordering within the melt.

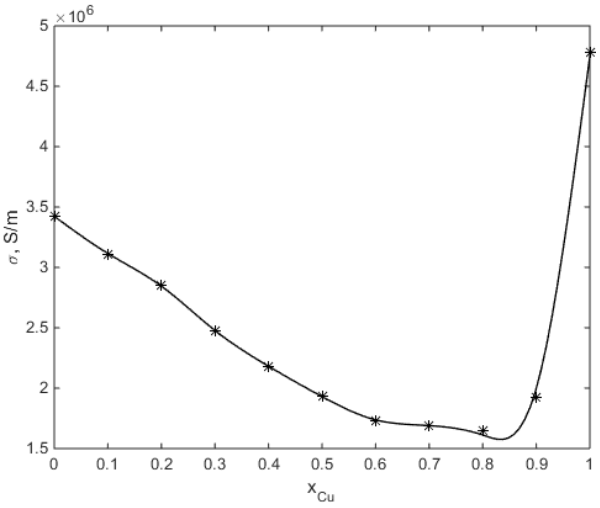

Figure 14: Copper-aluminium conductivity at 1373 K (1100 °C), calculated as inverse of the resistivity reported in [63].

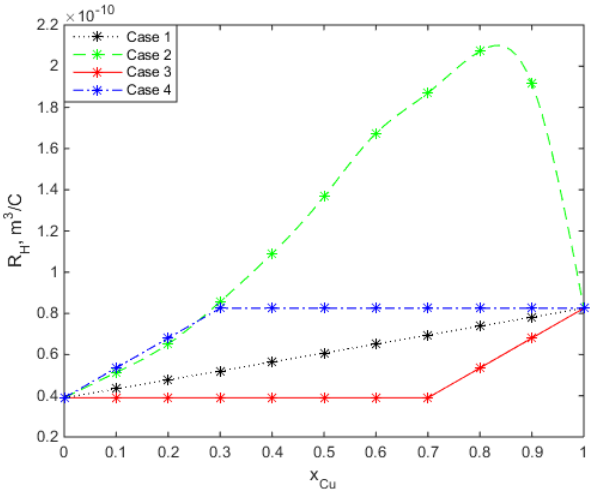

Figure 15: Hall effect coefficient estimated at 1373 K (1100 °C) from endmembers [64]– see text for case definitions.

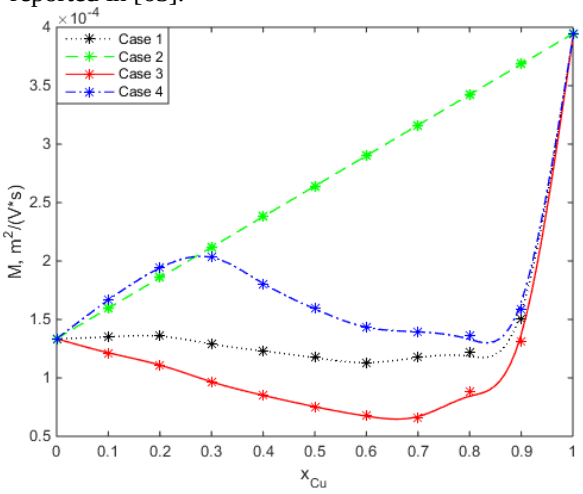

Figure 16: Hall mobility at 1373 K (1100 °C) estimated from end-members [64]– see text for case definitions.

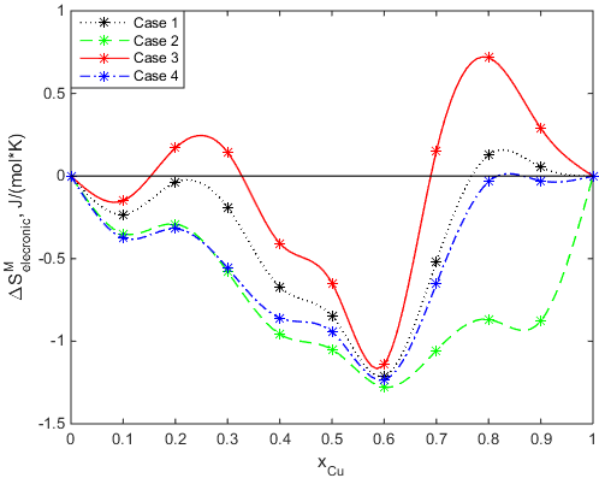

Figure 17: Electronic entropy of mixing at 1373 K (1100 °C) calculated from Seebeck [63], conductivity [63], and estimated Hall mobility.

The existence of ordering in melts has previously been correlated with increase viscosity for compositions where associate complexes are present[66,67], explaining the observed peak in viscosity near 50 to 70 mol% Cu. The source of the peak in viscosity near 10 to 25 mol% Cu is not readily apparent, but could suggest the presence of other associates, emphasizing the need for dedicated experimental research surrounding the structure of the liquid phase. Further research would aid in resolving discrepancy between Konstantinova[22] and Schick[13] in their reported composition of the aluminium-rich viscosity peak. Nevertheless, insight into liquid ordering is confirmed as being possible through electronic entropy of mixing. The later proves useful for describing peaks in viscosity of the copper-aluminium system,.

While integral total thermodynamic properties of mixing may mask specifics of phenomena such as ordering, measured thermodynamics from studies using EMF methods

indeed serve as a viable starting point for predicting general trends in liquid phase physical properties such as viscosity. A comparison of the dynamic viscosity calculated from our thermodynamic data using the Kozlov[56] and Schick-Brillo[20] models to literature values is depicted in Figure 19.

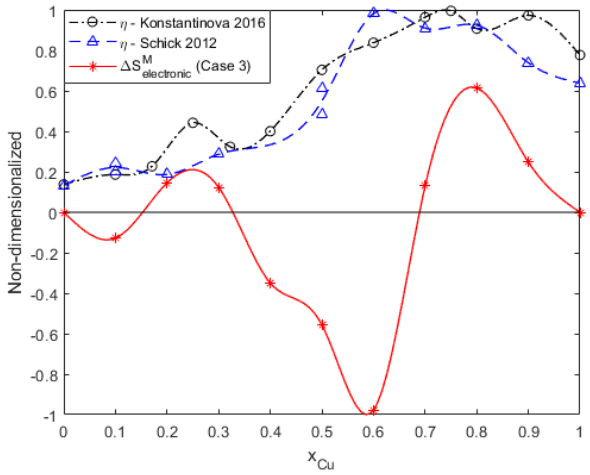

Figure 18: Comparison of experimental viscosities [13,22] and calculated electronic entropy of mixing at 1373 K (1100 °C). All curves are normalized to their maximum value

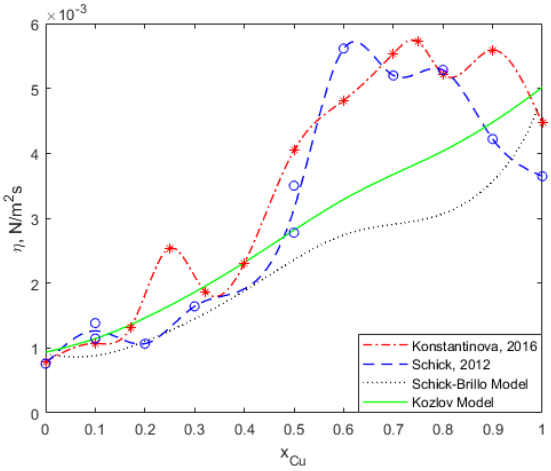

Figure 19: Viscosity calculated from electrochemical potential data at 1373 K (1100°C) using Kozlov and Shick-Brillo models, compared to experimental data [13,22].

The Kozlov model suggests an approximately linear relation between copper and aluminium viscosity. The Schick-Brillo model under-predicts the dynamic viscosity in the copper-rich region when experimental thermodynamic data is used, stemming from their implicit assumption that entropy of mixing for the copper-aluminium system is ideal, a claim disputed in this study and others[9,12,68].

Neither model reproduces the ordering-induced peaks in viscosity, presenting a shortcoming in current methods of thermophysical prediction of viscosity. Ordering shows a disproportionate effect on viscosity within a system, yet current methods of viscosity prediction from thermodynamics rely on activity or integral total mixing properties such as enthalpy, entropy, and Gibbs energy, all of which mask ordering effects in the liquid. A model based on thermodynamic phenomena such as electronic entropy that more readily illustrate the effects of ordering within a melt is necessary to accurately predict viscosity in systems exhibiting strong association. Currently, minimal experimental viscosity data exists for highly-ordered liquid alloy systems, hindering the development of such a viscosity model.

If viscosity is known or can be accurately calculated from thermodynamics, activity data can be used to predict self-diffusion coefficients within a melt using the Singh-Sommer relation[57] via Eqn(17,18). Calculated self-diffusion coefficients for copper and aluminium in copper-aluminium alloys are presented in Figure 20, both from experimental viscosity data and from viscosity calculated from EMF data via the Kozlov model for viscosity. While other experimental values for copper and aluminum self-diffusion are not present in the literature, values calculated using the Singh-Sommer relation and activity data are on the order of

magnitude expected for liquid copper and aluminium[69] and in acceptable agreement to recent *ab initio* molecular dynamic simulations[18] (*ab initio* MD). The peaks in experimental viscosity due to associates are manifested as troughs in calculated diffusion coefficients.

Overall the presence of ordering indicates that the Redlich-Kister solution model typically utilized[8,13,14] for CALPHAD is not appropriate for accurately describing the solution thermodynamics of strongly-ordered liquid alloy systems like copper-aluminium[70]. In addition such ordering also hinders the use of current thermophysical models for use in the determination of physical properties of a melt from thermodynamic data. For the purposes of accurately predicting liquid melt properties, the implementation of computational models that reflect non-ideal phenomena such as ordering are necessary.

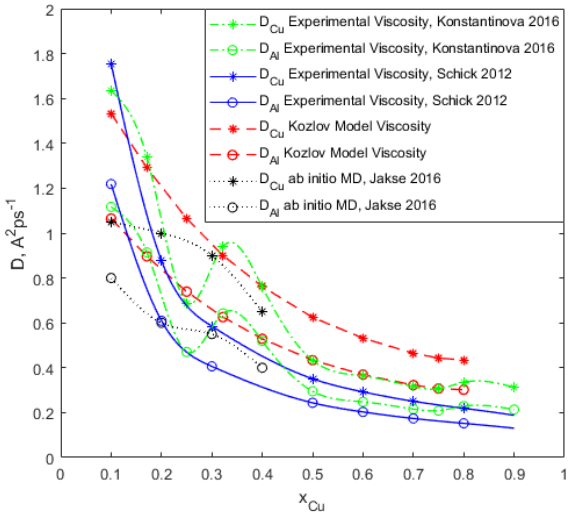

Figure 20: Diffusivities estimated from activity measured using the present electrochemical potential data at 1373 K (1100 °C) and experimental viscosity data [13,22], compared to *ab initio* MD results [18]

Conclusion

Copper(I) β" alumina (Cuβ"Al_2O_3) was synthesized through sintering, ion exchange, and melt-based methods. Utilizing electrochemical potential difference method, Cuβ"Al_2O_3 was successfully used to measure the thermodynamic of mixing of the copper-aluminium system, providing data in agreement with prior studies. It demonstrated the potential for use of Cuβ"Al_2O_3 as a component of an electrochemical sensor for measuring copper content in liquid metal processing. Explanations for physical property trends and structure were discussed in the context of thermodynamics of mixing and ordering. Electronic entropy of mixing is confirmed as a possible mean to inform short range ordering, in the present case reflecting trends in viscosity for the copper-aluminium system. Cuβ"Al_2O_3 represents a strong candidate for sensing applications in copper-aluminium alloys due to its electrochemically-predictable behavior with copper-aluminum melts, ease in synthesis and machining, and stability under air and at temperatures inherent to liquid metal processing.

Acknowledgements

The authors wish to acknowledge the MIT UROP Office and the Sanders, Lord, and DeFlorez UROP Funds for their financial support to this project. The authors wish to thank Mr. Andrew Caldwell, Ms. Jaclyn Leigh Cann, Mr. Brian Chmielowiec, Dr. Katsuhiro Nose, and Dr. Youyang Zhao for their insight and assistance.

Works Cited

1 M.T. Di Giovanni, E. Cerri, T. Saito, S. Akhtar, P. Åsholt, Y. Li, and M. Di Sabatino:

Metall. Ital., 2016, vol. 108, pp. 43–7.

2 R.A. Gonçalves and M.B. da Silva: *Procedia Manuf.*, 2015, vol. 1, pp. 683–95.

3 B. Upton: *Corrosion*, 1963, vol. 19, p. 204t–209t.

4 Y. Li, T.L. Ngai, and W. Xia: *Wear*, 1996, vol. 197, pp. 130–6.

5 M. Založnik, B. Sarler, and D. Gobin: *Mater. Tehnol.*, 2004, vol. 38, pp. 249–55.

6 G. Gaustad, E. Olivetti, and R. Kirchain: *Resour. Conserv. Recycl.*, 2012, vol. 58, pp. 79–87.

7 S.R. Wagstaff: *J. Sib. Fed. Univ. Eng. Technol.*, 2018, vol. 11, pp. 409–18.

8 N. Saunders: in *COST 507 Definition of thermochemical and thermophysical properties to provide a database for the development of new light alloys*, I. Ansara, A.T. Dinsdale, and M.H. Rand, eds., vol. 2, 1998, pp. 28–33.

9 A.I. Zaitsev, R.Y. Shimko, N.A. Arutyunyan, and S.F. Dunaev: *Dokl. Phys. Chem.*, 2007, vol. 414, pp. 115–9.

10 H. Oyamada, T. Nagasaka, and M. Hino: *Mater. Trans. JIM*, 1998, vol. 39, pp. 1225–9.

11 D.S. Kanibolotsky, O.A. Bieloborodova, N. V Kotova, and V. V Lisnyak: *J. Therm. Anal. Calorim.*, 2002, vol. 70, pp. 975–83.

12 U.K. Stolz, I. Arpshofen, F. Sommer, and B. Predel: *J. Phase Equilibria*, 1993, vol. 14, pp. 473–8.

13 M. Schick, J. Brillo, I. Egry, and B. Hallstedt: *J. Mater. Sci.*, 2012, vol. 47, pp. 8145–52.

14 V.T. Witusiewicz, U. Hecht, S.G. Fries, and S. Rex: *J. Alloys Compd.*, 2004, vol. 385, pp. 133–43.

15 A.S. Roik, V.P. Kazimirov, and V.E. Sokol'skii: *Russ. Metall.*, 2014, vol. 2014, pp. 23–32.

16 J. Brillo, A. Bytchkov, I. Egry, L. Hennet, G. Mathiak, I. Pozdnyakova, D.L. Price, D. Thiaudiere, and D. Zanghi: *J. Non. Cryst. Solids*, 2006, vol. 352, pp. 4008–12.

17 J. Dziedzic, S. Winczewski, and J. Rybicki: *Comput. Mater. Sci.*, 2016, vol. 114, pp. 219–32.

18 N. Jakse and A. Pasturel: *Phys. Rev. B*, 2016, vol. 94, pp. 1–13.

19 P. Dinsdale and P.N. Quested: *J. Mater. Sci.*, 2004, vol. 9, pp. 7221–8.

20 J. Schmitz, J. Brillo, I. Egry, and R. Schmid-Fetzer: *Int. J. Mat. Res.*, 2009, vol. 100, pp. 1529–35.

21 A.R. Kurochkin, P.S. Popel, D.A. Yagodin, A. V Borisenko, and A. V Okhapkin: *High Temp.*, 2013, vol. 51, pp. 224–32.

22 N.Y. Konstantinova, A.R. Kurochkin, A. V. Borisenko, V. V. Filippov, and P.S. Popel':

Russ. Metall., 2016, vol. 2016, pp. 144–9.

23 A.M. Vora: *Phys. Chem. Liq.*, 2008, vol. 46, pp. 213–22.

24 R.M. Khusnutdinoff, A.V. Mokshin, S.G. Menshikova, A.L. Beltyukov, and V.I. Ladyanov: *J. Exp. Theor. Phys.*, 2016, vol. 122, pp. 859–68.

25 M. V. Vaghela, a. Y. Vahora, N.K. Bhatt, B.Y. Thakore, and A.R. Jani: *AIP Conf. Proc.*, 2013, vol. 1536, pp. 637–8.

26 Y. Plevachuk, V. Sklyarchuk, A. Yakymovych, S. Eckert, B. Willers, and K. Eigenfeld: *Metall. Mater. Trans. A Phys. Metall. Mater. Sci.*, 2008, vol. 39, pp. 3040–5.

27 Z. Wen, J. Cao, Z. Gu, X. Xu, F. Zhang, and Z. Lin: *Solid State Ionics*, 2008, vol. 179, pp. 1697–701.

28 H. Kuwamoto and H. Sato: *Solid State Ionics*, 1981, vol. 5, pp. 187–8.

29 N. Weber: *Energy Convers.*, 1974, vol. 14, pp. 1–8.

30 T.K. Hunt, N. Weber, and T. Cole: *Solid State Ionics*, 1981, vol. 5, pp. 263–5.

31 S.M. Jeter: *Energy*, 1987, vol. 12, pp. 163–70.

32 D.J. Fray: *Met. Trans. B*, 1977, vol. 8B, pp. 153–6.

33 J. Liu and W. Weppner: *Solid State Commun.*, 1990, vol. 76, pp. 311–3.

34 J. Vangrunderbeek, F. Vandecruys, and R. V. Kumar: *Solid State Ionics*, 2000, vol. 136–137, pp. 567–71.

35 G. Dorner, H. Durakpasa, P. Linhardt, and M.W. Breitter: *Electrochim. Acta*, 1991, vol. 36, pp. 563–8.

36 R. Kvachkov, A. Yanakiev, C.N. Poulieff, P.D. Yankulov, S. Rashkov, and E. Budevski: *Solid State Ionics*, 1982, vol. 7, pp. 151–5.

37 R.J. Baughman and R.A. Lefever: *Mater. Res. Bull.*, 1975, vol. 10, pp. 607–12.

38 M.S. Whittingham and R.A. Huggins: *J. Electrochem. Soc.*, 1971, vol. 118, pp. 1–6.

39 J. Briant and G. Farrington: *J. Electrochem. Soc.*, 1981, vol. 128, pp. 1830–4.

40 G.M. Crosbie and G.J. Tennenhouse: *J. Am. Ceram. Soc.*, 1982, vol. 65, pp. 187–91.

41 Y. Yu Yao and J.T. Kummer: *J. Inorg. Nucl. Chem.*, 1967, vol. 29, pp. 2453–75.

42 J.A. Little and D.J. Fray: *Electrochim. Acta*, 1980, vol. 25, pp. 957–64.

43 T. Oishi, S. Tagawa, and S. Tanegashima: *J. Phys. Chem. Solids*, 2005, vol. 66, pp. 251–5.

44 J.A. Little and D.J. Fray: *Trans. Inst. Min. Metall.*, 1979, vol. 88, pp. C229–33.

45 J.D. Barrie, B. Dunn, O.M. Stafsudd, and P. Nelson: *J. Lumin.*

46 B. Cleaver and A. Davies: *Electrochim. Acta*, 1973, vol. 18, pp. 733–9.

47 S.K. Kim: *J. Korean Ceram. Soc.*, 1995, vol. 32, pp. 1040–6.

48 H. Kim, D.A. Boysen, D.J. Bradwell, B. Chung, K. Jiang, A.A. Tomaszowska, K. Wang, W. Wei, and D.R. Sadoway: *Electrochim. Acta*, 2012, vol. 60, pp. 154–62.

49 M.D. Koretsky: *Engineering and Chemical Thermodynamics*, 2nd edn., John Wiley & Sons Inc., 2013.

50 M.-L. Saboungi, W. Geertsma, and D.L. Price: *Annu. Rev. Phys. Chem.*, 1990, vol. 41, pp. 207–44.

51 M. Saboungi, J. Marr, and M. Blander: *J. Chem. Phys.*, 1978, vol. 68, pp. 1375–84.

52 C.C. Rinzler and A. Allanore: *Philos. Mag.*, 2016, vol. 96, pp. 3041–53.

53 H. Eyring: *J. Chem. Phys.*, 1936, vol. 4, pp. 283–91.

54 T. Tanaka, K. Hack, and S. Hara: *MRS Bull.*, 1999, vol. 24, pp. 45–9.

55 S. Seetharaman and D. Sichen: *Metall. Mater. Trans. B*, 1994, vol. 25, pp. 589–95.

56 J. Brillo: *Thermophysical Properties of Multicomponent Liquid Alloys*, Walter de Gruyter GmbH & Co KG, Berlin, 2016.

57 R.N. Singh and F. Sommer: *Phys. Chem. Liq.*, 1998, vol. 36, pp. 17–28.

58 H.A. Dabkowska, A.B. Dabkowski, R. Hermann, J. Priede, and G. Gerbeth: in *Handbook of Crystal Growth: Bulk Crystal Growth: Second Edition*, 2014.

59 J.L. Murray: Al-Cu Binary System.

60 G.H. Teichert, N.S.H. Gunda, S. Rudraraju, A.R. Natarajan, B. Puchala, K. Garikipati, and A. Van der Ven: *Comput. Mater. Sci.*, 2017, vol. 128, pp. 127–39.

61 C. Wagner: *Thermodynamics of Alloys*, Addison-Wesley Press, Inc, Cambridge, MA, USA, 1952.

62 M. Trybuła, N. Jakse, W. Gąsior, and A. Pasturel: *Arch. Metall. Mater.*, 2015, vol. 60, pp. 649–55.

63 J.-L. Bretonnet, J. Auchet, and J.G. Gasser: *J. Non. Cryst. Solids*, 1990, vol. 117–118, pp. 395–8.

64 H.U. Kunzi and H. Guntherodtf: in *The Hall Effect and its Applications*, C.L. Chien and C.R. Westgate, eds., Springer Science+Business Media, New York, NY, 1980, pp. 215–52.

65 S. Takeuchi and K. Murakami: *Sci. Reports Res. Institutes, Tohoku Univ. Ser. A, Physics, Chem. Metall.*, 1974, vol. 25, pp. 73–86.

66 S. Glasstone, K.J. Laider, and H. Eyring: *The Theory of Rate Processes; The Kinetics of Chemical Reactions, Viscosity, Diffusion, and Electrochemical Phenomena*, McGraw-Hill, 1941.

67 R.E. Aune, M. Hayashi, and S. Sridhar: *Ironmak. Steelmak.*, 2005, vol. 32, pp. 141–50.

68 O. Kubaschewski and C.B. Alcock: *Metallurgical Thermochemistry*, 5th edn., Pergamon Press, 1979.

69 T. Ejima and T. Yamamura: *J. Phys. Colloq.*, 1980, vol. 41, pp. C8-345-C8-348.

70 H.L. Lukas, S.G. Fries, and B. Sundman: *Computational Thermodynamics: The Calphad Method*, Cambridge University Press, New York, NY, 2007.

Appendix 1: Example of Raw OCP Data

Depicted below is an example of open circuit potential (OPC) data collected for $Cu_{0.4}Al_{0.6}$ vs Cu utilizing the copper-selective beta" alumina ($Cu\beta"Al_2O_3$) solid electrolyte described in this study. At a given temperature and composition, steady state in OCP readings was achieved within 1800 seconds. Typical standard deviations (sd) in OCP across a measurement period ranged from 0.02 to 2 mV, increasing with higher temperatures.

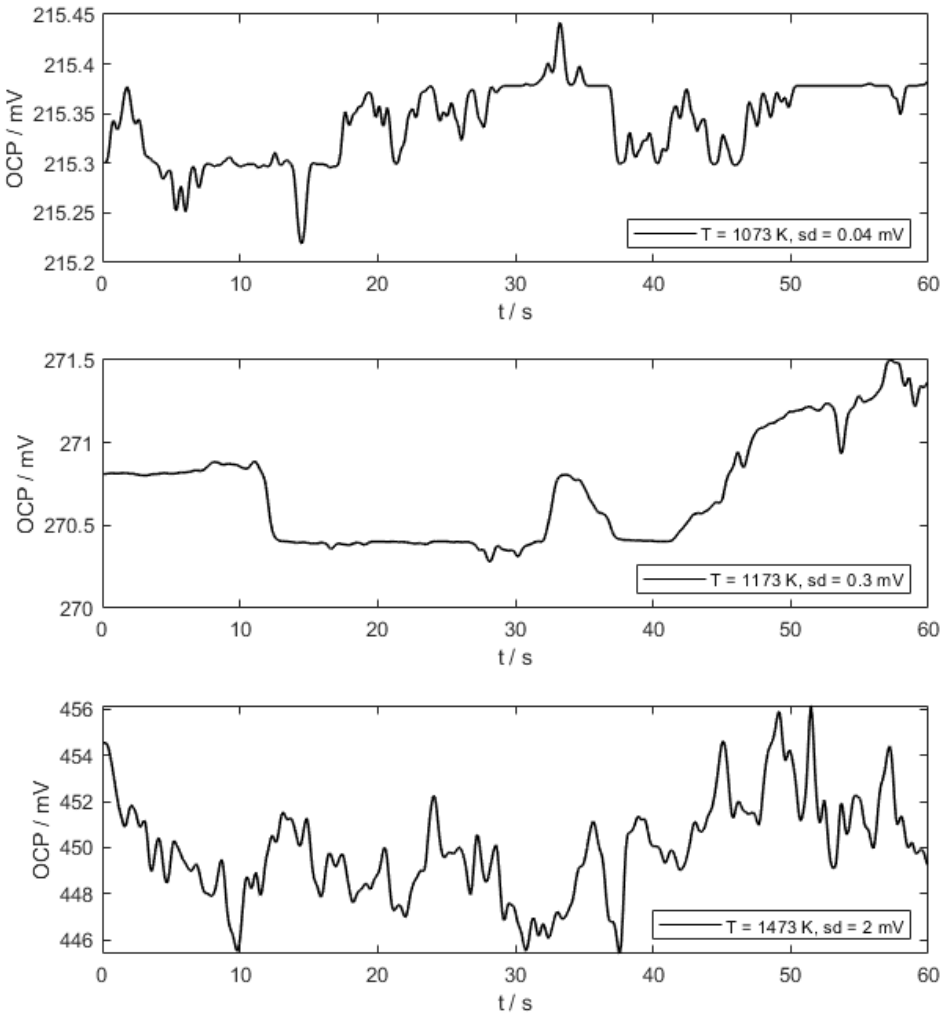

Figure A1: Sample of OCP data for $Cu_{0.4}Al_{0.6}$ referenced to Cu collected utilizing $Cu\beta"Al_2O_3$ after a stabilization period of 1800 s at each temperature.

Appendix 2:

Table AI. Summary of Thermodynamic Values

Summary of Copper-Aluminium Thermodynamics						**Units**
x_{Cu}	**0.1**	**0.2**	**0.4**	**0.6**	**0.8**	
T = 1473 K						
a_{Cu}	0.00125	0.00557	0.0273	0.163	0.583	
a_{Al}	0.859	0.667	0.336	0.0529	0.00288	
ΔG^M	-9.86	-16.7	-25.7	-27.7	-19.6	kJ/mol
ΔG^M_{Cu}	-81.8	-63.6	-44.1	-22.2	-6.61	kJ/mol
ΔG^M_{Al}	-1.87	-4.96	-13.4	-36.0	-71.6	kJ/mol
T = 1423 K						
a_{Cu}	0.00118	0.00517	0.0261	0.160	0.597	
a_{Al}	0.862	0.671	0.333	0.0511	0.00251	
ΔG^M	-9.56	-16.2	-25.1	-27.1	-19.1	kJ/mol
ΔG^M_{Cu}	-79.8	-62.3	-43.1	-21.7	-6.11	kJ/mol
ΔG^M_{Al}	-1.75	-4.72	-13.0	-35.2	-70.9	kJ/mol
T = 1373 K						
a_{Cu}	0.00111	0.00477	0.0249	0.157	0.612	
a_{Al}	0.866	0.676	0.330	0.0493	0.00216	
ΔG^M	-9.25	-15.8	-24.4	-26.4	-18.5	kJ/mol
ΔG^M_{Cu}	-77.7	-61.0	-42.1	-21.1	-5.61	kJ/mol
ΔG^M_{Al}	-1.64	-4.48	-12.7	-34.4	-70.1	kJ/mol
ΔH^M	-1.18	-3.82	-8.07	-8.56	-4.05	kJ/mol
ΔH^M_{Cu}	-21.3	-26.1	-15.1	-6.30	8.16	kJ/mol
ΔH^M_{Al}	1.05	1.76	-3.38	-11.9	-52.9	kJ/mol
ΔS^M	5.76	8.63	11.8	13.0	10.2	J/(mol*K)
ΔS^M_{Cu}	41.1	25.4	19.7	10.8	10.0	J/(mol*K)
ΔS^M_{Al}	1.84	4.43	6.57	16.3	11.1	J/(mol*K)
ΔS^M_{Excess}	3.06	4.47	6.22	7.41	6.08	J/(mol*K)
T = 1323 K						
a_{Cu}	0.00103	0.00437	0.0237	0.154	0.629	
a_{Al}	0.870	0.680	0.327	0.0473	0.00184	
ΔG^M	-8.94	-15.3	-23.8	-25.8	-17.9	kJ/mol
ΔG^M_{Cu}	-75.7	-59.8	-41.2	-20.6	-5.11	kJ/mol
ΔG^M_{Al}	-1.53	-4.24	-12.3	-33.6	-69.3	kJ/mol

Summary of Copper-Aluminium Thermodynamics					**Units**
x_{Cu}	**0.1**	**0.2**	**0.4**	**0.6**	
			T = 1273 K		
a_{Cu}	0.000955	0.00399	0.0225	0.151	
a_{Al}	0.888	0.695	0.332	0.0451	
ΔG^{M}	-8.486	-14.8	-23.1	-25.1	kJ/mol
ΔG^{M}_{Cu}	-73.6	-58.5	-40.2	-20.0	kJ/mol
ΔG^{M}_{Al}	-1.252	-3.852	-11.7	-32.8	kJ/mol
			T = 1173 K		
a_{Cu}	0.000805	0.00323	0.0199	-	
a_{Al}	0.911	0.715	0.334	-	
ΔG^{M}	-7.768	-13.8	-21.7	-	kJ/mol
ΔG^{M}_{Cu}	-69.5	-55.9	-38.2	-	kJ/mol
ΔG^{M}_{Al}	-0.910	-3.276	-10.7	-	kJ/mol
			T = 1073 K		
a_{Cu}	0.000657	0.00252	0.0172	-	
a_{Al}	0.917	0.725	0.321	-	
ΔG^{M}	-7.233	-13.0	-20.6	-	kJ/mol
ΔG^{M}_{Cu}	-65.4	-53.4	-36.2	-	kJ/mol
ΔG^{M}_{Al}	-0.773	-2.872	-10.1	-	kJ/mol
			T = 973 K		
a_{Cu}	0.000514	0.00186	0.0145	-	
a_{Al}	0.925	0.737	0.306	-	
ΔG^{M}	-6.70	-12.1	-19.4	-	kJ/mol
ΔG^{M}_{Cu}	-61.3	-50.9	-34.3	-	kJ/mol
ΔG^{M}_{Al}	-0.635	-2.47	-9.57	-	kJ/mol

Appendix 3: List of Symbols

a	Activity
c	Molar concentration
D	Self-diffusion coefficient
E	Cell potential difference
E^A	Activation energy for viscous flow
ES	Excess stability
F	Faraday constant
$\bar{H}$	Partial molar enthalpy
k_B	Boltzmann's constant
M	Hall mobility
r	Radius of diffusing particle
R	Ideal gas constant
R_H	Hall effect coefficient
$\bar{S}$	Partial molar entropy
$S_{CC}(0)$	Bhatia-Thornton structure factor
S^E	Electronic entropy
T	Absolute temperature
x	Mole fraction
$\bar{Y}$	Partial molar quantity
z	Number of electrons per copper (I) ion that travels across the Cuβ"Al_2O_3 membrane
α	Seebeck coefficient
ΔG^M	Gibbs energy of mixing
ΔH^M	Enthalpy of mixing
ΔS^M	Entropy of mixing
η	Dynamic viscosity
η^∞	Pre-exponential factor for viscous flow
μ	Partial molar Gibbs energy

σ	Electrical conductivity

List of Figures and Captions:

Figure 1: Electrochemical cell for exchange of Na^+ with Cu^+ in β''-Al_2O_3

Figure 2: Electrochemical potential measurement cell - geometry 1

Figure 3: Electrochemical potential measurement cell - geometry 2

Figure 4: Cuβ" Al_2O_3 synthesized directly from Cu_2O, MgO, and Al_2O_3 powders sintering

Figure 5: Cuβ"Al_2O_3 synthesized through ion exchange with Naβ"Al_2O_3 synthesized from $NaAlO_2$, MgO, and Al_2O_3 powders sintering

Figure 6: Cuβ"Al_2O_3 synthesized directly from melt of Cu_2O, MgO, and Al_2O_3

Figure 7: Variation of the electrochemical potential, referenced to liquid copper, with temperature and for 5 compositions (solid lines shows reproducible temperature range, dashed lines extend to the liquidus reported in [59])

Figure 8: Copper and aluminium activity evaluated at 1373K, compared to literature values [9-12]. Lines are spline fit interpolation of the present data, and aluminium activity estimated from Gibbs-Duhem eqn(5)

Figure 9: Gibbs energy of mixing estimated from electrochemical potential data (lines are spline fit interpolations)

Figure 10: Enthalpy of mixing at 1373 K (1100 °C) calculated by fitting the potential data to the Gibbs-Helmoltz relation (line is a spline fit interpolation)

Figure 11: Total (top star, plain line) and excess (star, dashed line) entropy of mixing at 1373 K (1100 °C) calculated by fitting the potential data to the Gibbs-Helmoltz relation (lines are spline fit interpolation). Plain bottom curve is the ideal (random) entropy of mixing

Figure 12: Excess stability (ES) calculated from experimentally determined thermodynamic properties of mixing, using Eqn(6) at 1373 K (1100 °C). Line is calculated from a spline fit interpolation of excess Gibbs energy of mixing

Figure 13: Bhatia-Thornton structure factor ($S_{CC}(0)$) at 1373 K (1100 °C) evaluated from the excess stability evaluated from the present data, compared to the ideal case using Eqn(8-9). Line is calculated from the spline fit interpolation utilized for excess stability. Dashed curves represent results of computational models [62]

Figure 14: Copper-aluminium conductivity at 1373 K (1100 °C), calculated as inverse of the resistivity reported in [63]

Figure 15: Hall effect coefficient estimated at 1373 K (1100 °C) from endmembers [64]– see text for case definitions

Figure 16: Hall mobility at 1373 K (1100 °C) estimated from end-members [64]– see text for case definitions

Figure 17: Electronic entropy of mixing at 1373 K (1100 °C) calculated from Seebeck [63], conductivity [63], and estimated Hall mobility

Figure 18: Comparison of experimental viscosities [13,22] and calculated electronic entropy of mixing at 1373 K (1100 °C). All curves are normalized to their maximum value

Figure 19: Viscosity calculated from electrochemical potential data at 1373 K (1100°C) using Kozlov and Shick-Brillo models, compared to experimental data [13,22].

Figure 20: Diffusivities estimated from activity measured using the present electrochemical potential data at 1373 K (1100 °C) and experimental viscosity data [13,22], compared to *ab initio* MD results [18]

Figure A1: Sample of OCP data for $Cu_{0.4}Al_{0.6}$ referenced to Cu collected utilizing Cuβ"Al_2O_3 after a stabilization period of 1800 s at each temperature